Part II

Results of Calculations

Chapter 5

Exchange Mechanisms in Heusler Alloys

5.1 Introduction

As we have seen in preceding chapter Heusler alloys exhibit very rich magnetic behavior. One can study in the same family of alloys a series of interesting diverse magnetic phenomena like itinerant and localized magnetism, antiferromagnetism, helimagnetism, or non-collinear magnetism. This diverse magnetic behavior reflects the complex nature of exchange interactions in these systems. Depending on the number of magnetic atoms within the unit cell there can be several exchange mechanisms which coexist and are mixed together. For instance in some Mn-based systems where the total magnetic moment is confined to Mn sublattice an indirect exchange mechanism seems most probable due to large distance between Mn magnetic moments. Indeed, for these systems early model Hamiltonian based studies assuming an indirect exchange coupling (s-d) between the Mn atoms via conduction electrons provided a qualitative information on the nature of magnetism. On the other hand, we know that in several full Heusler alloys (X_2MnZ; X = Fe, Co, Ni, Rh) X atoms also carry a substantial magnetic moment. In this case things get more complicated since there will be many exchange interactions between different magnetic atoms each of which will contribute to the formation of the magnetic state in a cooperative manner. For example, magnetic properties of quaternary Heusler alloys NiCoMnSb with three different magnetic atoms within the unit cell is governed by at least six different exchange interactions.

Our objective in this chapter as well as in the following chapters is a comprehensive study of exchange interactions and Curie temperature in both families of Heusler alloys. The calculational methods both for the exchange interactions and finite temperature properties are introduced in chapters 2 and 3, respectively. An overview of the previous experimental and theoretical studies on these materials is given in chapter 4. For a general discussion it is convenient to divide Heusler alloys into two groups. First group contains the systems with one magnetic atom per unit cell. Almost all semi Heusler alloys as well as some Mn-based

full Heusler alloys enter this group. Compounds with more than one magnetic atom per unit cell are included in the second group. The magnetism of the systems within the first group is relatively easy to understand but still very interesting since they present a diverse magnetic behavior as mentioned above. On the basis of available experimental information and early model Hamiltonian calculations an indirect exchange coupling mechanism is proposed for the first group of systems. This model is also supported by parameter-free first-principles calculations of Kübler *et al* [58]. However, the situation is not so easy for the compounds in the second group. Thus, the understanding of magnetism in these systems constitutes one of the aims of the present thesis.

Our extensive investigations on the second group of systems showed that the magnetism in these systems is rather complicated. First, due to Friedel oscillations there is always an indirect exchange interaction among the magnetic atoms, which strongly depends on conduction electron concentration. Second, because of the small distances between Mn and X atoms there is also a considerable overlap of $3d$ wave functions of these atoms (direct exchange). This interaction can be ferromagnetic or antiferromagnetic depending on the filling of the $3d$ orbitals of the atoms. Co_2MnZ and Mn_2VZ compounds which will be studied in the next chapter are the best examples for the former and latter case, respectively. Another distinct feature of this interaction is that it strongly depends on the value of the magnetic moment of the X atom. For small values of the X magnetic moment (0.1-0.3 μ_B) this interaction plays a secondary role while it becomes extremely important with increasing X moment. The former case will be illustrated by the example of Ni_2MnZ compounds in the following section. Intermediate and large X moment limits will be considered in the next chapter.

In section 5.2 we discuss magnetism of the systems within the second group of alloys considering experimentally well known Ni_2MnZ compounds. Section 5.3 is devoted to a detailed study on the role of the conduction electrons in mediating exchange interactions between Mn atoms both in semi- and full-Heusler alloys from the first group. Many of the systems investigated in this thesis show half-metallic character. Due to the vital importance of these systems for spintronics applications the results for them are presented in a separate chapter (chapter 6).

5.2 Ni_2MnZ (Z = Ga, In, Sn, Sb) compounds

Recently these Ni-based Heusler alloys received tremendous experimental and theoretical interest because of the two unique properties that they exhibit: Shape memory effect and inverse magnetocaloric effect. In the preceding chapter we introduced shape memory effect. Shape memory alloys are promising materials for future applications. They can be used as sensors and actuators in different fields. The currently used materials (e.g. NiTi, CuAlNi alloys) use the temperature as a parameter to trigger the shape change. However, in ferromagnetic shape memory alloys magnetic field plays the same role as temperature. Thus,

Table 5.1: Experimental lattice parameters, magnetic moments (in μ_B) and mean-field estimation of the Curie temperatures for Ni_2MnZ (Z = Ga, In, Sn, Sb). Lattice parameters and the experimental Curie temperature values are taken from Ref.[50]

Compound	a(Å)	Mn	Ni	Z	Cell	$MFA_{[Mn\text{-}Mn]}$	$MFA_{[all]}$	Exp.
Ni_2MnGa	5.825	3.570	0.294	-0.068	4.090	302	389	380
		3.43[a]	0.36[a]	-0.04[a]	4.11[a]			
					4.17[b]			
Ni_2MnIn	6.069	3.719	0.277	-0.066	4.208	244	343	315
Ni_2MnSn	6.053	3.724	0.206	-0.057	4.080	323	358	360
		3.53[c]	0.24[c]	-0.03[c]	4.08[c]			
Ni_2MnSb	6.004	3.696	0.143	-0.033	3.950	343	352	365

[a]Ref.[85]
[b]Ref.[86] (Exp.)
[c]Ref.[87]

switching process can be made much faster and better controlled compared to conventional shape memory alloys. Among the ferromagnetic shape memory alloys Ni_2MnGa is the most studied one, it undergoes a magnetic phase transition at around 370 K and a martensitic phase transition at approximately 200 K. At the martensitic phase of Ni_2MnGa an applied field of about 1 T can induce strains as large as 10% [47, 48].

The inverse magnetocaloric effect (MCE) has its origin in a martensitic phase transformation that modifies the exchange interactions due to the change in the lattice parameters. For samples with compositions close to Ni_2MnZ (Z = Ga, Sn) stoichiometry an inverse MCE has been reported. This is an extrinsic effect arising from the coupling at the mesoscale between the martensitic and magnetic domains [78]. Applying a magnetic field adiabatically, rather than removing it as in ordinary MCE, causes the sample to cool. This is very important for room temperature refrigeration as an environment-friendly alternative to conventional vapor-cycle refrigeration. This has prompted intensive research in this field [79, 80, 81, 82].

In spite of substantial theoretical and experimental research aimed at understanding these two mechanisms, the study of exchange interactions in these systems received less attention. It is worth to note that the second effect (inverse MCE) is closely related to the distance dependence of the exchange interactions in these systems [82]. Recently Enkovaara *et al* studied the spin-spirals in Ni_2MnZ (Z = Al, Ga) and estimated Curie temperature from the calculated dispersions [83]. The authors showed that the Ni sublattice plays important role in the magnetic properties of the systems.

The main purpose of the present section is a detailed study of the exchange interactions in these systems. In particular we report a systematic study of the exchange interaction

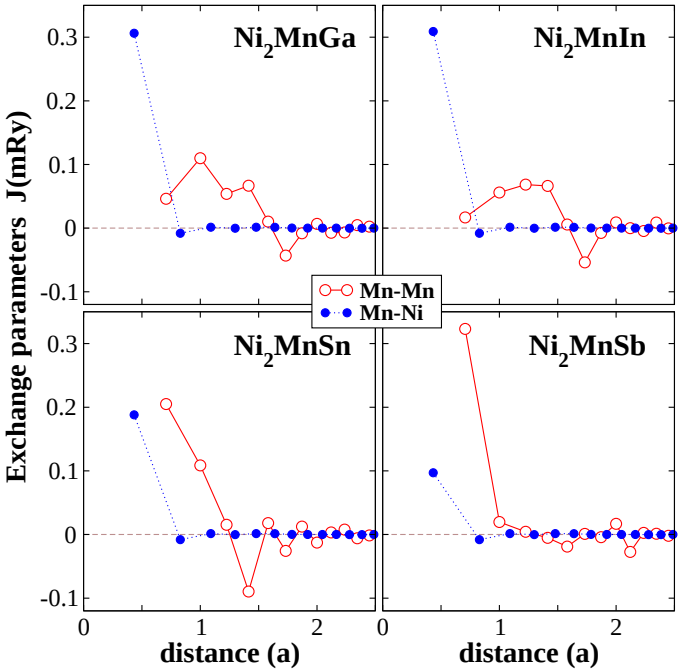

Figure 5.1: The parameters of the Mn-Mn (intra-sublattice) exchange interactions and Mn-Ni (inter-sublattice) exchange interactions in Ni_2MnZ (Z = Ga, In, Sn, Sb). The distances are given in the units of the lattice constant. The significance of the oscillations of the exchange parameters is verified by varying the **q** mesh in the frozen-magnon calculations.

between atoms of different sublattices and show that pattern of exchange interactions in these systems deviates strongly from the physical picture that can be expected on the basis of the experimental information available. Indeed common crystal structure, similar chemical composition and close experimental values of the Curie temperature make the assumption natural that the exchange interactions in these systems are similar. Our study shows, however, that this assumption is not correct [84]. The exchange interactions vary strongly depending on the Z constituent. In particular, the inter-sublattice interactions change strongly from system to system. We show that different exchange interactions lead, in agreement with experiment, to similar values of the Curie temperatures. We analyze the relation between the properties of the exchange interactions and the Curie temperatures.

- **Magnetic moments and exchange parameters**

In Table 5.1 we present calculated magnetic moments. For comparison, the available experimental values of the moments and the results of previous calculations are presented. Relative variation of the Mn moment is small. On the other hand, the moment of Ni and Z atoms show strong relative variation and are in Ni_2MnSb about two times smaller than in Ni_2MnGa or Ni_2MnIn. The values of the magnetic moments are in good agrement with the results of previous calculations.

The calculated Heisenberg exchange parameters are presented in Fig. 5.1. As mentioned in the introduction, the assumption that the closeness of the experimental Curie temperatures is the consequence of the similarity of the exchange interactions is not confirmed by the calculations. We obtain strong dependence of the exchange interactions on the type of the Z atom. For Z = Ga and Z = In that belong to the same column of the Mendellev's table (see

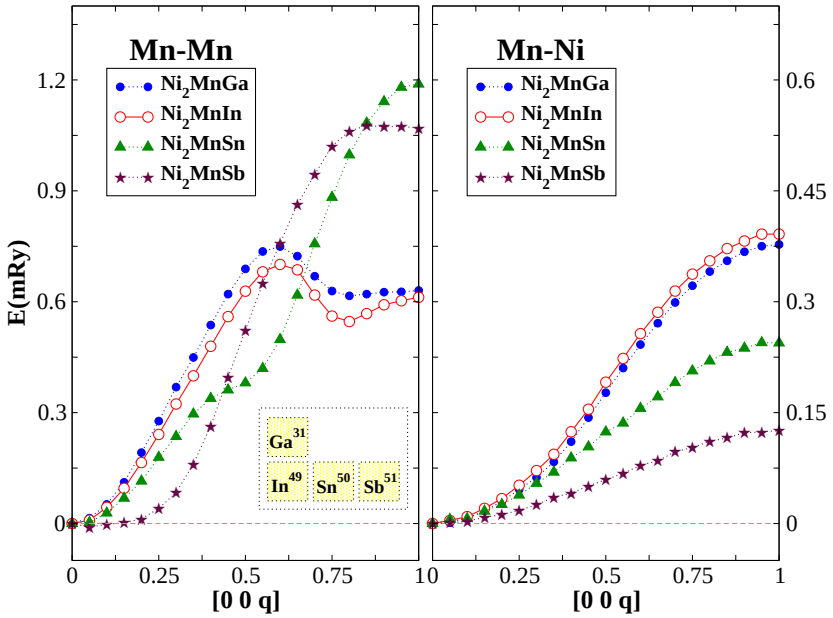

Figure 5.2: Frozen-magnon energies as a function of the wave vector **q** (in units of $2\pi/a$) in Ni_2MnZ for Mn-Mn (left) and Mn-Ni interactions (right).

inset in Fig. 5.2) we obtain similar pattern of Heisenberg exchange parameters. On the other hand, for Z atoms belonging to different columns the changes in the exchange interactions are very strong (Fig. 5.1). These changes concern both the Mn-Mn intra-sublattice interactions and the Ni-Mn inter-sublattice interaction.

Considering the Mn-Mn interactions we notice that in Ni_2MnGa and Ni_2MnIn the interaction with the coordination spheres from the first to the forth is positive. The interaction with the first coordination sphere is weaker than with the following ones. The interaction with the fifth sphere is very small. The interaction with the 6th sphere is negative. The interaction with further coordination spheres is very weak.

In Ni_2MnSn the interaction with the first sphere strongly increases compared with Ni_2MnGa and Ni_2MnIn. On the other hand, the interaction with the third sphere becomes small. The interaction with the forth sphere is strongly negative. The interaction with further neighbors are weak.

The trend observed in transition from Ni_2MnGa and Ni_2MnIn to Ni_2MnSn becomes even stronger in the case of Z = Sb. Here the interaction with the first neighbor increases further and is the only strong exchange interaction between the Mn atoms.

The inter-sublattice Mn-Ni interaction behaves very differently. A sizable direct interaction takes place only between nearest neighbors. This interaction is very strong in Ni_2MnGa and Ni_2MnIn and quickly decreases for Z = Sn and, especially, Z = Sb.

In spite of substantial experimental works on the structural and magnetic properties of Heusler alloys the information for the exchange interactions is very limited. Noda and Ishikawa [54] measured the spin wave spectra of Ni_2MnSn and Pd_2MnSn for various directions in the Brillouin zone and analyzed the results within the Heisenberg model. They found an long range and oscillatory character for the exchange interactions. Especially these oscillations were reaching beyond the the eight nearest neighbor distance in both compounds.

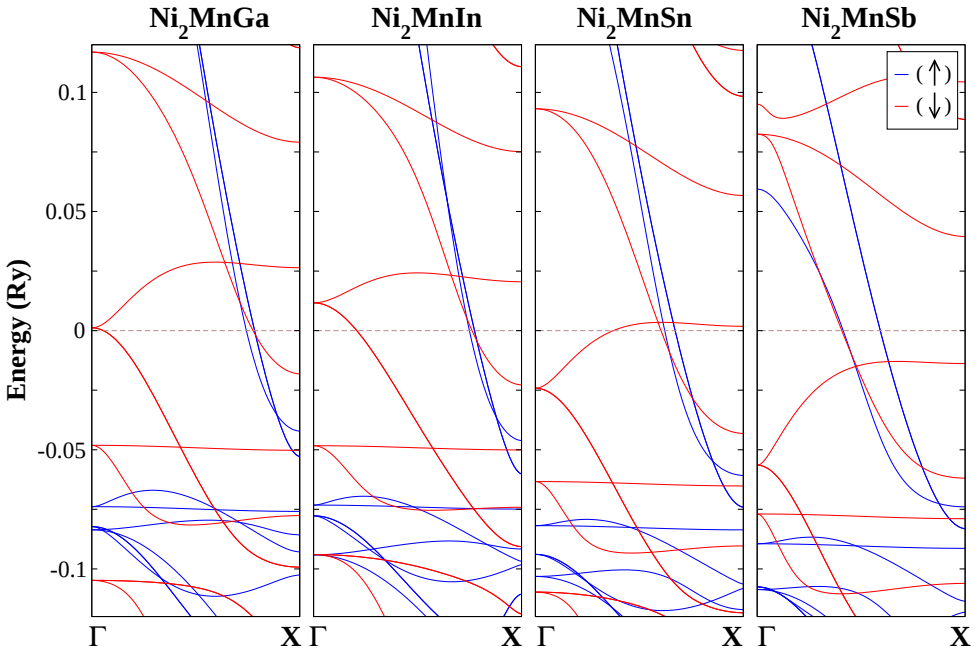

Figure 5.3: Band structure of Ni_2MnZ along the high symmetry line (Γ-X).

Interestingly, we obtained a very similar pattern of exchange parameters for Ni_2MnSn. Combining our theoretical findings with experimental results of Noda and Ishikawa we can draw a rough conclusion that exchange coupling in Mn-based Heusler alloys is indirect via the conduction electrons. A detailed analysis for the role of the conduction electrons in mediating exchange interactions will be given in the next section.

- **Frozen-magnon energies and band structure**

To reveal the physical origin of the strong difference in the exchange parameters of these systems we plot in Fig. 5.2 the frozen-magnon energies as a function of wave vector $\mathbf{q}$ for one direction in the Brillouin zone. The energy of the frozen magnon with a given $\mathbf{q}$ can be seen as a result of a complex interaction of the ferromagnetic states separated by vector $\mathbf{q}$ in the reciprocal space [6]. This interaction is stronger if the states have close energies and weaker for the states separated by a large energy interval. We remind the reader that the inter-atomic exchange parameters are Fourier transforms of the E($\mathbf{q}$) functions and therefore reflect their form. Indeed, E($\mathbf{q}$) curves for Ni_2MnGa and Ni_2MnIn are close to each other that leads to a similar set of interatomic exchange parameters (Fig. 5.1). These curves deviate strongly from a simple cosinusoid having a maximum at $\mathbf{q}$ about 0.6 and a rather weak variation at $\mathbf{q} > 0.6$. The complexity of E($\mathbf{q}$) means that several Fourier components are needed to describe the features of the function. This is reflected in the the Heisenberg's parameters of Ni_2MnGa and Ni_2MnIn.

On the other hand, the E($\mathbf{q}$) curve of Ni_2MnSb is well described by one cosinusoid (Fig. 5.2) that results in a single large Mn-Mn exchange parameter (Fig. 5.1). The E($\mathbf{q}$) of Ni_2MnSn

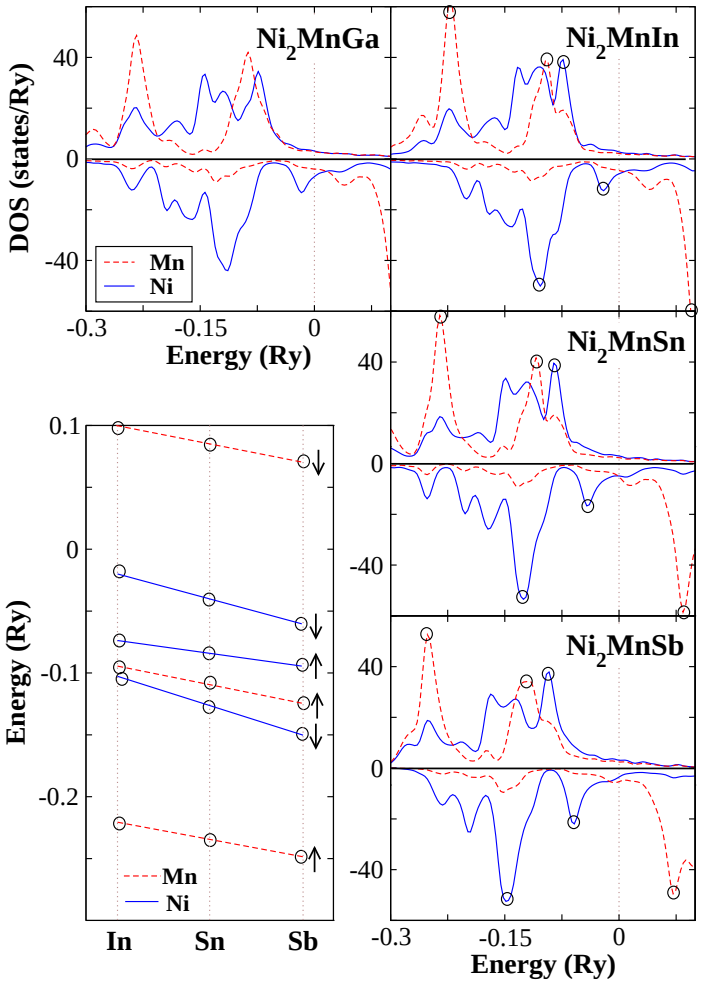

Figure 5.4: Spin-projected partial density of states of Ni_2MnZ. The separate graph in the left-hand bottom part of the figure shows the variation of the positions of a number of the DOS peaks for the In-Sn-Sb series of compounds. The lines in this graph are guides for the eye. The energies are measured with respect to the Fermi level of the corresponding system. The small open circles on the DOS curves mark the positions of the peaks. Arrows show spin projections. The analysis of the states at the Fermi level shows that the main contributions comes from the 3d states of Mn and Ni.

assumes an intermediate position from the viewpoint of the complexity of the function. This property is also reflected in the exchange parameters (Fig. 5.1).

- **Density of states and Curie temperature**

Note that the character of the **q**-dependence of the energy illustrated by Fig. 5.2 is a consequence of the properties of the electronic structure of the compounds. Indeed, in Fig. 5.3 we see that the electronic structures of Ni_2MnGa and Ni_2MnIn are similar. Transition along the row In-Sn-Sb leads to increasing difference in the electron spectrum. This increasing difference can be traced back to the change in the number of valence electrons: a Sb atoms has two more valence electrons than In and one more electron than Sn. As the result an important difference in the electron structure of the system is a relative shift of the Fermi level to a higher energy position in the sequence In-Sn-Sb. This shift is clearly seen in the DOS presented in Fig. 5.4. The positions of the same features of the DOS in different systems are well described by linear functions with negative angle coefficients. For the Mn peaks all three lines are almost parallel. This means that the change in the Mn DOS from system to system can be treated as a rigid shift with respect to the Fermi level. In the case of the Ni-

DOS the situation is more complicated since, besides the variation of the electron number, an additional influence on the peak positions is exerted by the variation of the Ni atomic moment (see Table 5.1).

The E($\mathbf{q}$) curves determining the Mn-Ni interactions are presented in Fig. 5.2. The form of the curves is in all cases close to a cosinusoid. Therefore, only one exchange parameter has sizable value. The strength of the interaction is in correlation with the value of the magnetic moment of the Ni atoms.

The interatomic exchange parameters are used to evaluate the Curie temperature. If only the Mn-Mn interactions are taken into account we obtain values shown in Table 5.1. Despite very strong difference in the Mn-Mn exchange parameters in these systems the difference in the corresponding Curie temperatures is not very large. The explanation for this result is the property that in MFA to a one-sublattice ferromagnet the value of the Curie temperature is determined by the sum of the interatomic exchange interactions $J_0 = \sum_{\mathbf{R}\neq 0} J_{0\mathbf{R}}$. J_0 gives the average value of E($\mathbf{q}$) and is less sensitive to the detailed form of the E($\mathbf{q}$) function.

The comparison of the Curie temperatures calculated with the use of the Mn-Mn exchange parameters only with experimental Curie temperatures shows that the agreement with experiment is not in general good. In the case of Ni_2MnGa the error is about 30%.

Account for inter-sublattice interactions improves the agreement with experimental T_C values considerably (Table 5.1). This shows that the Ni moment provides a magnetic degree of freedom which plays important role in the thermodynamics of the system.

5.3 Role of the conduction electrons in mediating exchange interactions between Mn atoms

Our studies on experimentally well established Ni-based compounds in the preceding section revealed a complex character of the magnetism in these systems. In particular, long range and oscillatory behavior of the exchange interactions as well as their strong dependence on the Z constituent gave an evidence for the conduction electron mediated exchange interactions in Heusler alloys. Also, as we have seen in the preceding chapter an indirect exchange coupling model was used to interpret the observed spin wave spectra of several Heusler alloys. The first DFT calculations of the exchange interactions by Kübler *et al.* for a number of full Heusler alloys gave a strong support for the above indirect exchange coupling model.

To gain further insight into the role of the conduction electrons in exchange coupling we performed a systematic study on several Mn-based semi- and full Heusler alloys going beyond the stoichiometric compositions. In particular, we focus on the systems in which total magnetic moment is confined to Mn sublattice in order to avoid further complexities due to the additional exchange interactions between different magnetic atoms. These systems also provide a great simplification in calculations and subsequent interpretation of the results. Several Heusler compounds of XYZ and X_2YZ type satisfy above condition if X element is chosen from the late transition metals (i.e., Cu, Pd, Ag, Pt, Au). Among them especially Pd-

Table 5.2: Experimental lattice parameters in X_kMnZ (X = Pd, Cu; k = 1, 2; Z = In, Sn, Sb, Te) for stoichiometric compositions. The last column gives the lattice constants used in calculations which are obtained by taking the average of lattice constants in sequence In-Sn-Sb-Te for experimentally existing compounds.

Compound	$a_{[In]}$(Å)	$a_{[Sn]}$(Å)	$a_{[Sb]}$(Å)	$a_{[Te]}$(Å)	$a_{[Z]}$(Å)
PdMnZ	-	-	6.25	6.27	6.26
CuMnZ	-	-	6.09	-	6.09
Pd_2MnZ	6.37	6.38	6.41	-	6.38
Cu_2MnZ	6.20	6.17	-	-	6.18

and Cu-based stoichiometric full Heusler compounds Pd_2MnZ (Z=In, Sn, Sb) and Cu_2MnZ (Z=In, Sn) and non-stoichiometric ones $Pd_2MnZ_{1-x}Z'_x$ [(Z,Z′)=(In, Sn), (Sn, Sb), (In, Sb)] and $Cu_2MnIn_{1-x}Sn_x$ received huge experimental interest. Early measurements by Webster *et al.* on quaternary full Heusler alloys $Pd_2MnIn_{1-x}Sn_x$ demonstrated the importance of the conduction electrons in establishing magnetic properties [50]. Recent experiments on quaternary semi Heusler compounds $Ni_{1-x}Cu_xMnSb$ and $AuMnSn_{1-x}Sb_x$ gave even more interesting results which reveal the decisive role of the conduction electron number in magnetic order and phase transition temperature T_C [88, 89].

We consider Pd and Cu containing Mn-based semi and full Heusler alloys which is expressed in compact a form as $X_kMnZ_{1-m}Z'_m$ [X = Pd, Cu; k = 1, 2; (Z, Z′)=(In, Sn), (Sn, Sb), (Sb, Te); $0 \leq m \leq 1$]. We use the virtual crystal approximation (VCA) to vary electron concentration. Half of the considered systems are not studied experimentally and thus their lattice constants are not known. As it is seen from Table 5.2 one or two compounds exist experimentally from semi-Heusler compounds and more in the case of full Heusler compounds. Therefore we use only an average lattice constant in the sequence In-Sn-Sn-Te. (see Table 5.2). This is a good approximation since, as we know from experiments, Heusler alloys containing different *sp*-atoms from the same row of Periodic Table have similar lattice parameters [50, 51]. Indeed, as it is seen in Table 5.2 the maximum variation of the lattice parameters from In to Te is less than 1%. An important increase is observed in transition from $3d$ to $4d$ systems due to large size of the $4d$ atoms.

Going beyond the stoichiometric compositions provided very important information on the nature of magnetism especially for semi Heusler alloys. For these systems we obtain a strong dependence of the exchange interactions on the number of the valence electrons. The systems with the same number of valence electrons, like PdMnSn and CuMnIn, have qualitatively similar patterns of exchange parameters and, as a result, similar Curie temperatures. We find a clear relationship between the strength of the exchange interactions and the conduction electron polarization. The larger the conduction electron polarization the stronger the exchange interactions. For zero polarization the calculated Curie temperature

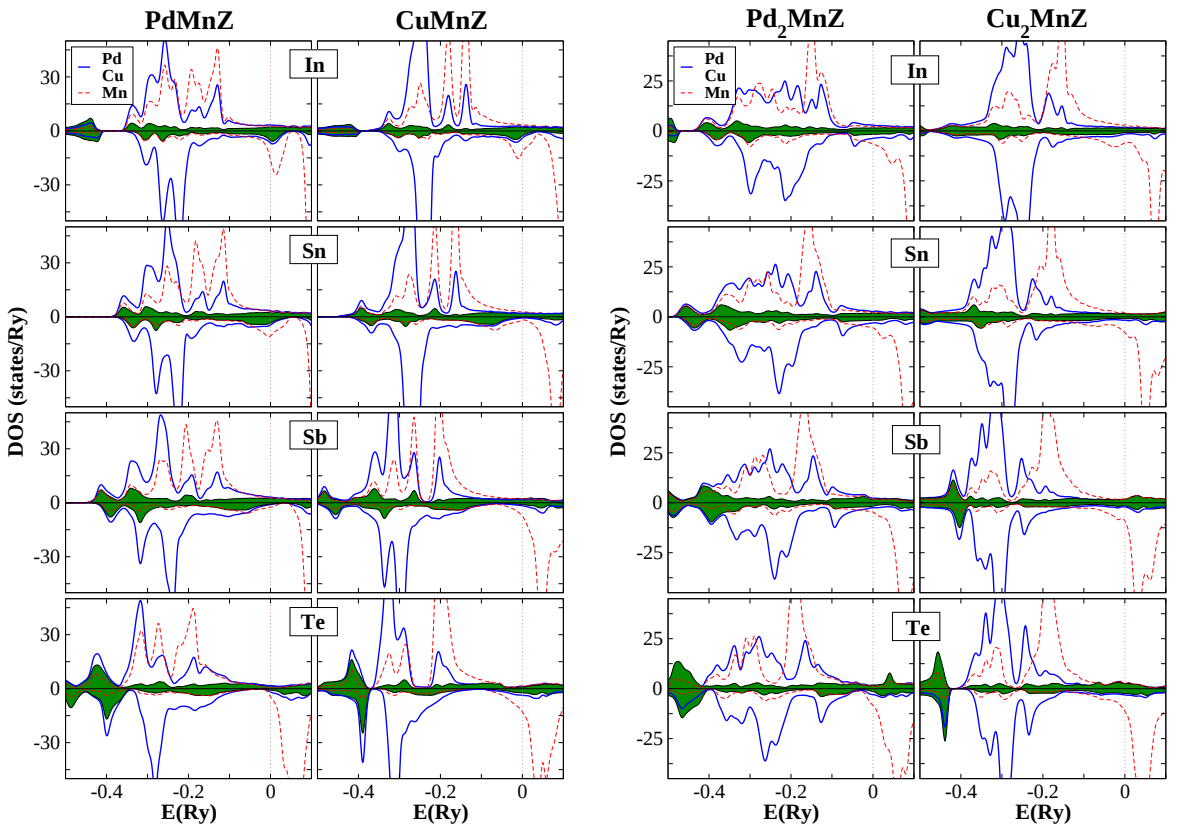

Figure 5.5: Left panel: Spin-projected atom-resolved density of states of PdMnZ and CuMnZ (Z=In, Sn, Sb, Te) for stoichiometric compositions. With shaded green color we show the DOS of Z constituent. The broken vertical lines denote the Fermi level. Left panel: The same for full Heusler compounds Pd_2MnZ and Cu_2MnZ.

also vanishes. However, the situation is not so evident for full Heusler alloys. We find a qualitative correlation between conduction electron polarization and Curie temperature but no relation between the exchange interactions for the systems with same number of valance electrons like Cu_2MnIn and Pd_2MnSb. In both families of systems the calculated exchange parameters are quite long range that indicates an indirect coupling between Mn atoms via the conduction electrons.

In last part of this section we investigate the role of $3d$ and $4d$ atoms in exchange coupling by comparing the results for Ni_2MnZ and Pd_2MnZ (Z=In, Sn, Sb, Te) for two different lattice parameters. Our calculations showed that $3d$ or $4d$-atoms have practically no effect on mediation of the exchange interactions. Magnetism of both systems appeared to be strongly depending on the Z constituent and conduction electron polarization. For the same Z constituent we obtain a similar pattern of exchange interactions in the case of almost equal conduction electron polarizations.

- **Density of states and magnetic moments**

In Fig. 5.5 we present the atom resolved density of states of X_kMnZ (X = Pd, Cu; k = 1, 2;

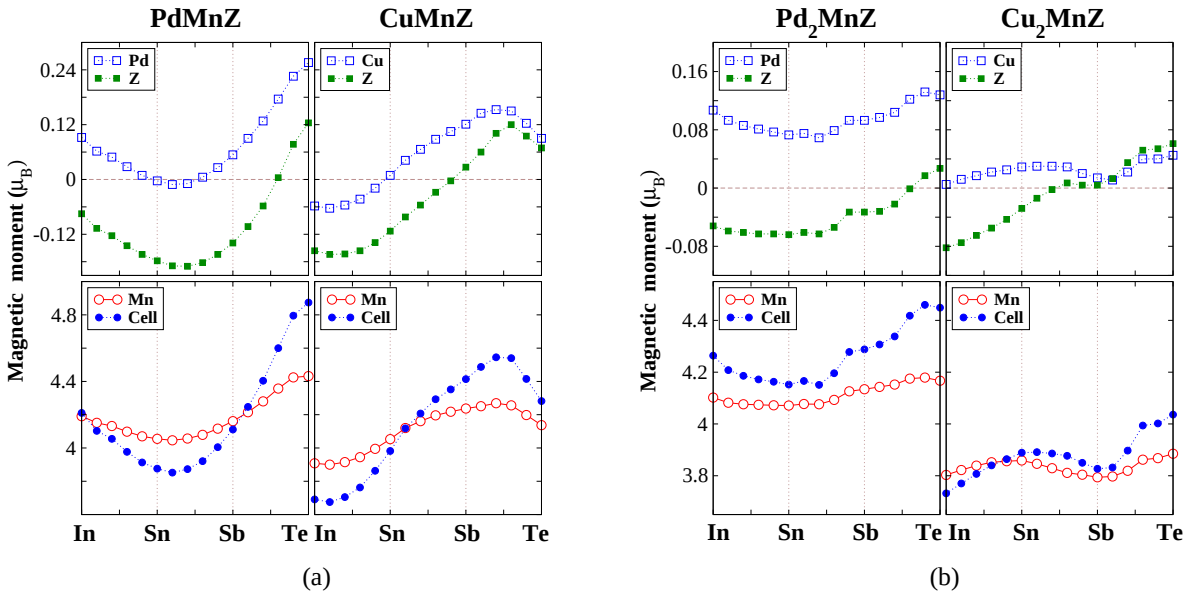

Figure 5.6: (a) Calculated atom-resolved and total spin moments (in μ_B) in PdMnZ and CuMnZ as a function of the *sp*-electron number of the Z constituent. (b) The same for full Heusler alloys Pd_2MnZ and Cu_2MnZ.

Z = In, Sn, Sb, Te) for stoichiometric compositions. In agreement with the commonly accepted picture of magnetism for Mn-based Heusler alloys we obtain a strong localization of magnetization on the Mn sublattice with a value of magnetic moment close to $4\mu_B$. The localized nature of magnetism will be further discussed in the next subsection. An important difference in the electron structure of these compounds is a relative shift of the Fermi level to a higher energy position in sequence In-Sn-Sb-Te due to change of the number of valance electrons within the same row of Periodic Table. This shift is clearly seen in the DOS presented in Fig. 5.5. Note that a Sb atom has two more valence electrons than In, one more electron than Sn and one less electron then Te. The DOS for semi-Heusler compounds show an interesting feature that different compositions give similar behavior if the total number of the *sp* electrons coming from different atoms is equal. This similarity is more pronounced near Fermi level. For example the peaks in Mn spin down states of PdMnSn and CuMnIn are very much similar to each other. This distinct feature of the DOS for semi-Heusler alloys is related to the symmetry properties of the wave functions in $C1_b$-type crystal structure [67, 68].

In Fig. 5.7 we present calculated atom resolved and total magnetic moments in both family of Heusler alloys PdMnZ, CuMnZ, Pd_2MnZ and Cu_2MnZ as a function of the *sp*-electron number of the Z constituent. As mentioned above, the magnetic moment is mostly confined to Mn sublattice. A small induced moment is found on Cu and Pd sublattices which is positive in a broad composition interval while this moment is negative for Z constituent. An interesting observation in Z dependent properties of the induced moments is that they almost follow the behavior of the Mn moment from In to Te. This correlation is more

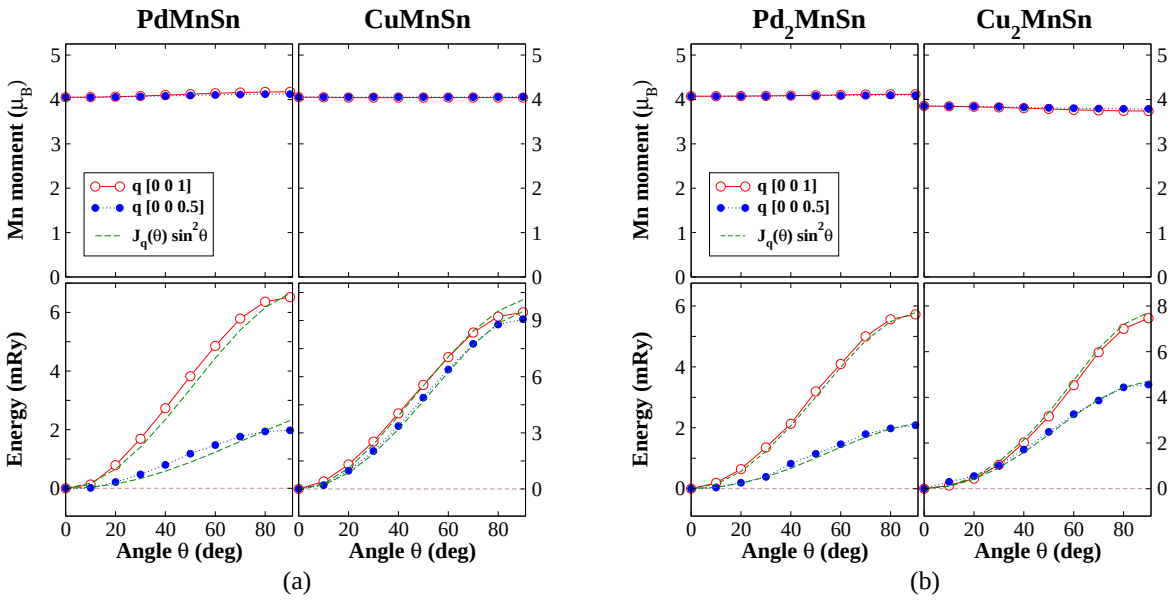

Figure 5.7: (a) Upper panel: Calculated Mn spin moment in PdMnSn and CuMnSn as a function of θ for spin spiral with $\mathbf{q} = (0\,0\,\frac{1}{2}), (0\,0\,1)$ in units of π/a. Lower panel: Corresponding total energies $\Delta E(\theta, \mathbf{q}) = E(\theta, \mathbf{q}) - E(0, 0)$. For comparison results of force theorem (broken lines) is presented. $\mathrm{J}_{\mathbf{q}}(\theta)$ stand for $\mathrm{J}_{\mathbf{q}} \times M_\theta^2$, M is the magnetic moment. (b) The same for Pd_2MnSn and Cu_2MnSn full Heusler compounds.

pronounced in semi-Heusler alloys (see Fig. 5.7). Furthermore, in semi Heusler compounds different compositions give similar values for magnetic moments with a small shift in the case of equal total number of valance electrons. This small shift stems from the different lattice constants. Additionally, the changes associated with total magnetic moment is very large in semi-Heusler compounds. In PdMnZ this is about 1 μ_B, half of it comes from the change in Mn magnetic moment. On the other hand, the situation is different in full Heusler alloys, neither a correlation nor a substantial change in magnetic moments is obtained.

5.3.1 Local moment behavior

As we have seen in preceding chapter Mn-based Heusler compounds are considered to be ideal local moment systems on the basis of experimental information available. This feature was theoretically confirmed by early DFT calculations of Kübler *et al.* for a number of full Heusler compounds [58]. Considering PdMnSn, CuMnSn, Pd_2MnSn and Cu_2MnSn from semi and full Heusler compounds as a prototype we calculated magnetic moments an total energies as a function of θ for spin spiral with two different $\mathbf{q}$ values chosen in z direction and compare the relative stability of the different magnetic configurations. Note that spin spiral technique allows one to treat all possible magnetic configurations between ferromagnetic and antiferromagnetic states. Here we restrict ourselves to the two $\mathbf{q}$ values: $\mathbf{q} = (0\,0\,\frac{1}{2})$ and $\mathbf{q} = (0\,0\,1)$. θ angle varied between 0 and 90. Note also that spin spiral having $\theta = 0$ with any value of $\mathbf{q}$ and $\theta = 90$ with $\mathbf{q} = (001)$ corresponds to ferromagnetic and antiferromagnetic

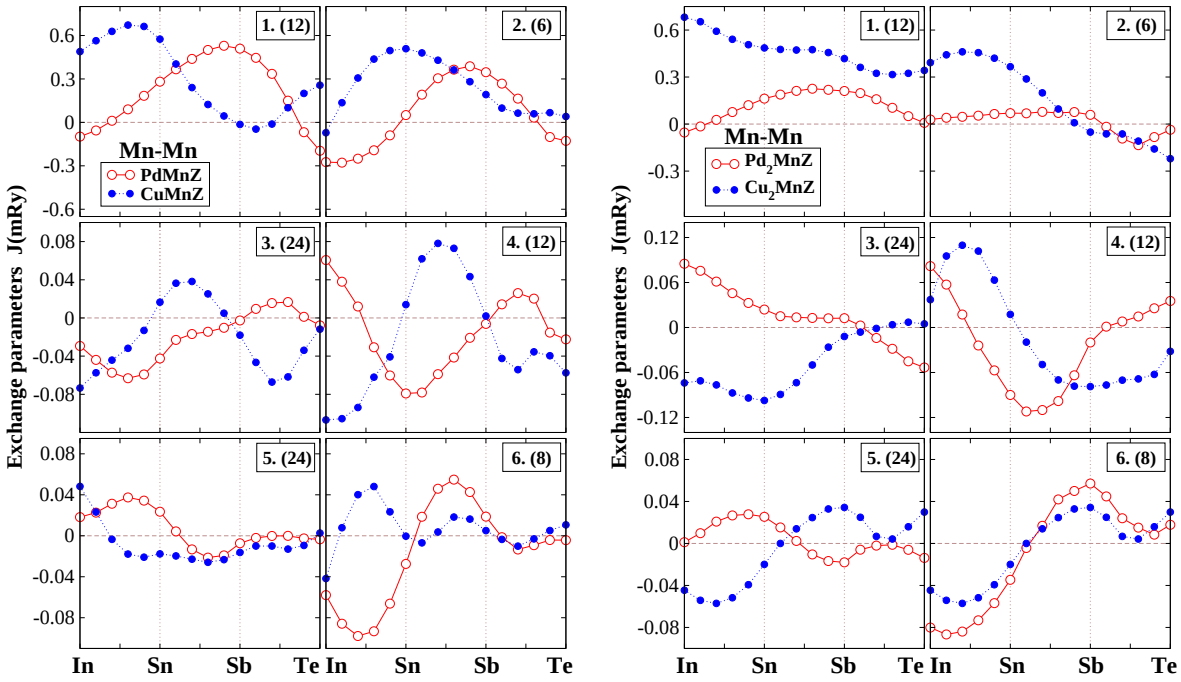

Figure 5.8: Left panel: First six nearest neighbor Mn-Mn exchange parameters in PdMnZ and CuMnZ as a function of the *sp*-electron number of the Z constituent. Also given are the number of atoms within corresponding coordination spheres. Right panel: The same for full Heusler alloys Pd_2MnZ and Cu_2MnZ.

states, respectively.

The obtained results are presented in Fig. 5.7. For all considered systems the magnetic moment of the Mn atom is practically insensitive to the type of the magnetic ordering. The relative change of the Mn moment in transition from ferromagnetic to antiferromagnetic state is less than 3%. On the other hand, the calculated total energy increases with increasing θ angle and reaches the maximum value for $\theta = 90$ with $\mathbf{q} = (0\,0\,1)$ that corresponds to antiferromagnetic phase. This shows that ground state is ferromagnetic in all cases. The obtained stability of the magnetic moments reflects the localized nature of magnetism in both family of Heusler alloys as well as justifies the approach used in calculation of exchange parameters. Furthermore, the agreement between calculated values of $\Delta E(\theta, \mathbf{q})$ and $J_{\mathbf{q}}(\theta)\sin^2\theta$ implies the possibility of using large angles ($30 < \theta < 90$) in calculation of exchange parameters in local moment systems which is not usually the case for $3d$ transition metals.

5.3.2 Indirect exchange coupling

In Fig. 5.8 we present calculated first six nearest neighbor Mn-Mn exchange parameters for both families of compounds as a function of *sp*-electron concentration together with number of atoms within corresponding coordination spheres. Behavior of the same quantities for larger distances ($\sim 10\,a$) is given in Fig. 5.9 for selected compounds PdMnIn, CuMnIn, Pd_2MnIn

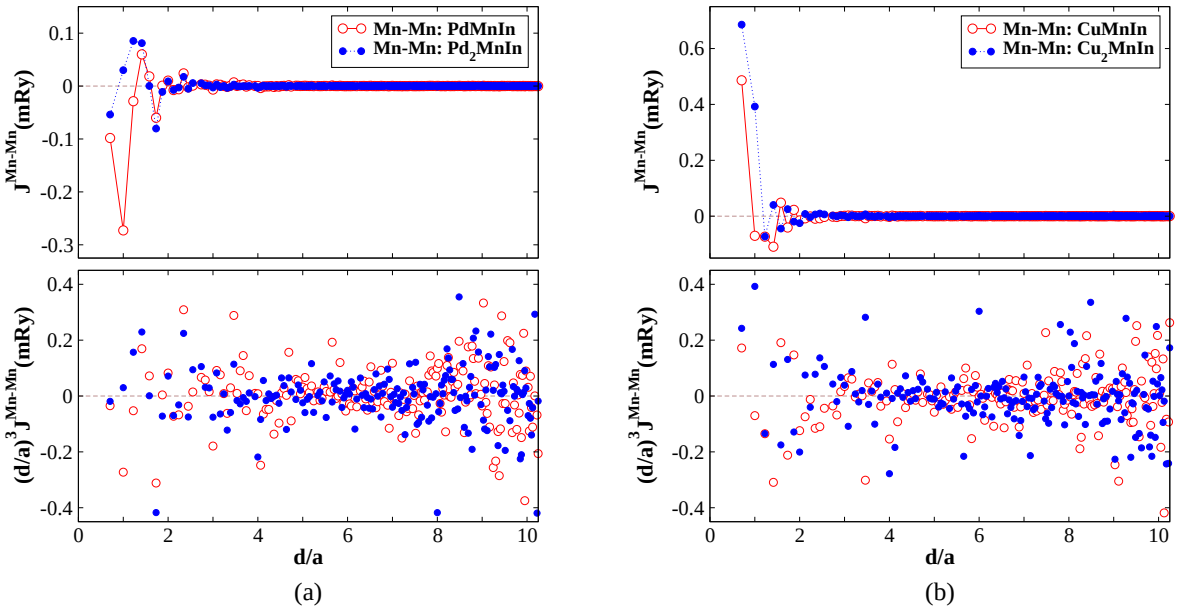

Figure 5.9: (a) Upper panel: Mn-Mn exchange interactions in Pd_kMnIn (k = 1, 2) as a function of distance up to the $10a$. Lower panel: RKKY-type oscillations in exchange parameters for corresponding compounds. (b) The same for Cu_kMnIn (k = 1, 2).

and Cu_2MnIn. As it is seen from Figs. 5.8 and 5.9 the Mn-Mn interactions are long-ranged reaching beyond the 6th nearest neighborhood distance and have the RKKY-type oscillating character. The absolute value of the parameters decays quickly with increasing interatomic distance and the main contribution to T_C comes from the interaction between atoms lying closer than $3a$. No sizable contribution is detected after $5a$. Nevertheless, even at very large distances RKKY-type oscillations becomes visible when exchange parameters are multiplied by $(d/a)^3$ (see Fig. 5.9) that reveal the indirect exchange coupling in these systems mediated by conduction electrons.

In agreement with the results of preceding section we obtain a strong dependence of the exchange parameters on the Z constituent for both families of Heusler compounds. As it is seen from Fig. 5.8 all exchange parameters oscillates between ferromagnetic and antiferromagnetic values with increasing *sp*-electron concentration. These oscillations are related to the detailed electron structure of the systems. Considering first two nearest neighbor exchange parameters we see that they have ferromagnetic character for a broad composition range and dominate over the rest of the parameters. The remaining ones are very weak and have similar energy dependencies. Note that it is these first two nearest neighbor exchange interactions which give rise to very high Curie temperatures in Cu-based full Heusler alloys as well as both classes of semi Heusler alloys. Furthermore, we obtain a strong correlation between strength of the exchange interactions and *sp*-electron (conduction electron) polarization (see Fig. 5.10). The larger the conduction electron polarization the stronger the obtained exchange parameters.

A distinct feature of the magnetism in semi-Heusler alloys is that the maximum of the

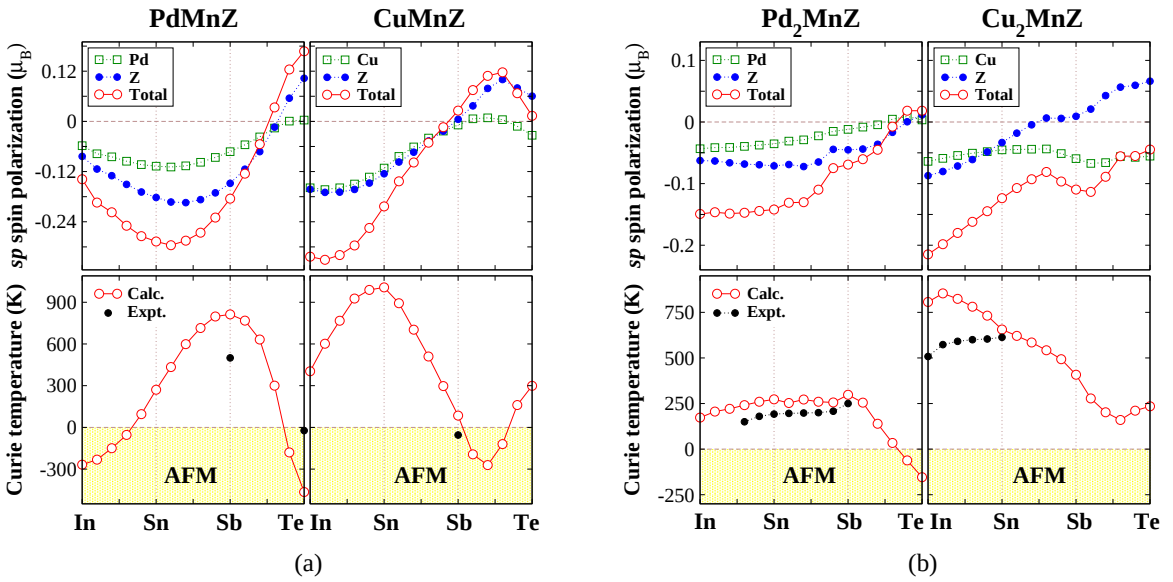

Figure 5.10: (a) Upper panel: The *sp*-electron spin polarization (in μ_B) of the X=Pd,Cu and Z constituents. The total polarization is given as the sum of X and Z spin polarizations. Lover panel: Mean-field estimation of the Curie temperature in PdMnZ and CuMnZ. For comparison available experimental T_C values taken from Ref.[50] are presented. (b) The same for the full-Heusler alloys Pd_2MnZ and Cu_2MnZ.

exchange interactions for both PdMnZ and CuMnZ corresponds to the similar number of the *sp*-electrons. The shift of the maxima for two systems is explained by the fact that Pd has one *sp*-electron less than Cu. The properties of the exchange interactions are reflected in the properties of the Curie temperature (see Fig. 5.10) where we also obtained a relative shift of the maxima of the two curves corresponding to one *sp*-electron. On the other hand, no such correlation is obtained for the full Heusler compounds.

5.3.3 Conduction electron polarization and Curie temperature

The problem of interaction between local moments and resulting Curie temperature is rather closely connected with the problem of conduction electron polarization around a magnetic moment. To clarify this issue it is important to obtain information on the conduction electron spin polarization. In Fig. 5.10 we present calculated *sp*-electron spin polarization and Curie temperatures for both families of Heusler alloys. For both classes of systems we obtain a qualitative correlation between the spin polarizations and Curie temperatures. In particular the systems with vanishing *sp*-electron spin polarization are characterized by the value of the Curie temperature that is very close to zero. Also, large spin polarization gives rise to high T_C values in both families of alloys. Additionally, the sign of the spin polarization gives information on the nature of magnetic structure. For negative spin polarizations we obtain a ferromagnetic order in a large interval of compositions while positive polarization results in an antiferromagnetic order. A non-collinear magnetic structure is obtained for

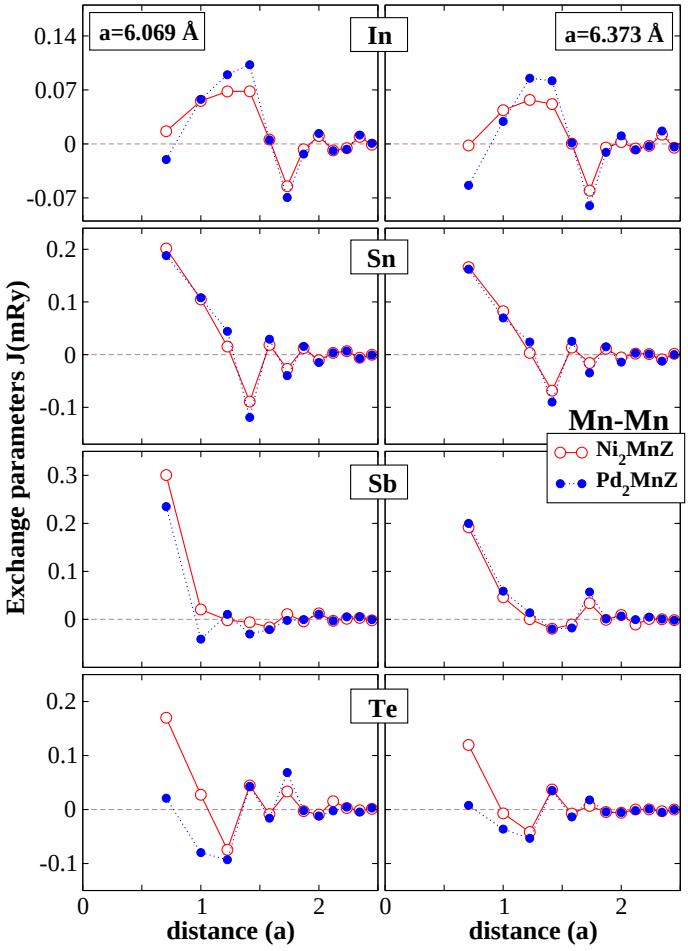

Figure 5.11: The parameters of the Mn-Mn exchange interactions in Ni_2MnZ and Ni_2MnZ (Z=In, Sn, Sb, Te) for two different lattice constants.

vanishing values of *sp*-electron spin polarization. These properties reveal the decisive role of the *sp*-electrons of the X and Z atoms in mediating the exchange interaction between the Mn spin moments as well as magnetic ordering. This makes spin-polarization of the *sp*-electrons important parameter for tuning the value of the Curie temperature in these systems. The obtained values of Curie temperatures are in good agreement with the available experimental data (see Fig. 5.10).

The first experimental information on the conduction electron polarization of Heusler alloys is provided by measurement and analysis of the hyperfine fields in non-magnetic sites (X,Z) in these systems. The strength of the transferred hyperfine fields correlates with the amplitude of the *s*-electron polarization. Indeed measurements by Campbell and Khoi *et al.,* shoved that maximum conduction electron polarization is found in systems with high Curie temperatures such as Cu_2MnAl and Cu_2MnIn [74, 75]. Recently, Zukowski *et al.,* using Compton scattering profiles, obtained a large conduction electron spin polarization in Cu_2MnAl which is antiferromagnetically coupled to Mn moment [76]. Also, a similar result is obtained for Ni_2MnSn by Deb *et al.,*[77]. Our calculations are in agreement with these recent experiments.

Table 5.3: Magnetic moments and *sp*-electron polarization (in μ_B) in Ni_2MnZ and Pd_2MnZ (Z = In, Sn, Sb, Te) for two different lattice parameters.

	$a = 6.07$ Å					$a = 6.37$ Å				
Compound	X	Mn	Z	*sp*	Cell	X	Mn	Z	*sp*	Cell
Ni_2MnIn	0.27	3.72	-0.07	-0.16	4.19	0.27	3.99	-0.07	-0.17	4.45
Pd_2MnIn	0.11	3.81	-0.05	-0.14	3.98	0.17	4.10	-0.05	-0.15	4.26
Ni_2MnSn	0.21	3.74	-0.06	-0.13	4.10	0.21	4.00	-0.06	-0.14	4.35
Pd_2MnSn	0.09	3.79	-0.06	-0.13	3.91	0.07	4.07	-0.06	-0.14	4.15
Ni_2MnSb	0.15	3.76	-0.03	-0.09	4.04	0.22	4.04	-0.02	-0.06	4.46
Pd_2MnSb	0.08	3.82	-0.03	-0.08	3.95	0.09	4.13	-0.03	-0.07	4.29
Ni_2MnTe	0.22	3.83	0.03	0.01	4.31	0.21	4.04	0.02	-0.03	4.48
Pd_2MnTe	0.14	3.89	0.04	0.04	4.21	0.13	4.17	0.03	0.02	4.45

5.3.4 $3d$ versus $4d$ electrons

The role of the *sp*-electrons in mediating exchange interactions is further emphasized by a correlation between exchange parameters of different systems with a similar polarization. Fig. 5.11 present the exchange parameters of Ni_2MnZ and Ni_2MnZ (Z=In, Sn, Sb, Te) for two different lattice spacings. For each lattice parameter we obtain a similar pattern of exchange parameters for X=Ni and Pd also in the case of similar *sp*-electron spin polarizations (see Table 5.3). As it is seen from Table 5.3 and Fig. 5.11 this similarity is more pronounced for Ni_2MnSn and Pd_2MnSn compounds that they have equal *sp*-electron spin polarizations. For both lattice parameters the strong deviations in exchange parameters occur in the case of Z=Te where also the conduction electron spin polarizations assume quite different values.

In conclusion, we have shown that the magnetism of the Heusler alloys is characterized by the complex pattern of the exchange interactions that cannot be predicted without direct calculation. On the other hand our calculations show that the magnetic properties of the broad classes of the Heusler alloys can be tuned by the variation of the number and spin-polarization of the *sp*-electrons. This finding suggests a practical tool for the design of the materials with given properties.